A Stiffness Switch in Human Immunodeficiency Virus

Nitzan Kol,* Yu Shi,† Marianna Tsvitov,* David Barlam,† Roni Z. Shneck,‡ Michael S. Kay,§ and Itay Rousso*
*Department of Structural Biology, Weizmann Institute of Science, Rehovot 76100, Israel; †Department of Mechanical Engineering and ‡Department of Materials Engineering, Ben-Gurion University of the Negev, Beer-Sheva 84105, Israel; and §Department of Biochemistry, University of Utah School of Medicine, Salt Lake City, Utah 84112-5650

ABSTRACT After budding from the cell, human immunodeficiency virus (HIV) and other retrovirus particles undergo a maturation process that is required for their infectivity. During maturation, HIV particles undergo a significant internal morphological reorganization, changing from a roughly spherically symmetric immature particle with a thick protein shell to a mature particle with a thin protein shell and conical core. However, the physical principles underlying viral particle production, maturation, and entry into cells remain poorly understood. Here, using nanoindentation experiments conducted by an atomic force microscope (AFM), we report the mechanical measurements of HIV particles. We find that immature particles are more than 14-fold stiffer than mature particles and that this large difference is primarily mediated by the HIV envelope cytoplasmic tail domain. Finite element simulation shows that for immature virions the average Young's modulus drops more than eightfold when the cytoplasmic tail domain is deleted (930 vs. 115 MPa). We also find a striking correlation between the softening of viruses during maturation and their ability to enter cells, providing the first evidence, to our knowledge, for a prominent role for virus mechanical properties in the infection process. These results show that HIV regulates its mechanical properties at different stages of its life cycle (i.e., stiff during viral budding versus soft during entry) and that this regulation may be important for efficient infectivity. Our report of this maturation-induced ''stiffness switch'' in HIV establishes the groundwork for mechanistic studies of how retroviral particles can regulate their mechanical properties to affect biological function.

INTRODUCTION

Retroviruses are complex self-assembled structures that are specifically designed to spread infection. The viral Gag protein alone is necessary and sufficient for production of virus-like particles (1). The other major structural protein of human immunodeficiency virus (HIV) particles is the envelope glycoprotein (Env, gp160). Env is synthesized as a precursor that is proteolytically cleaved into two subunits: a receptor-binding subunit (gp120) and a transmembrane subunit (gp41). The gp120/gp41 complex is required for receptor binding and viral entry (2–5). HIV and other lentiviruses differ from most retroviruses in that they have very long (~150 residue) Env cytoplasmic tails (CT). These CT domains have been shown to interact with the matrix (MA) region of Gag and are important for Env localization to sites of virus budding and efficient Env incorporation into virions (6–9). Mutations within the MA domain (4,8) and deletions in the gp160 CT domain (6,8,9) block Env incorporation into virions.

After budding from the cell, HIV and other retrovirus particles undergo a maturation process that is required for their infectivity. Virus maturation is induced by the enzymatic cleavage of the viral Gag protein by virus-encoded protease (PR) into three main structural proteins: MA, capsid (CA), and nucleocapsid (NC) (10) (Fig. 1 *A*). Viral maturation has been extensively studied using biochemical methods and a variety of electron microscopy (EM) imaging techniques. During maturation, HIV particles undergo a significant internal morphological reorganization, as observed by EM, changing from a roughly spherically symmetric immature particle with a thick protein shell to a mature particle with a thin protein shell and a prominent conical core (11) (schematically shown in Fig. 1 *B*).

Despite substantial progress in morphological and biochemical characterization of the virus life cycle, the physical principles underlying virus production, maturation, and entry into cells remain poorly understood. A virion must satisfy several potentially conflicting demands during its lifetime—spontaneous assembly during budding, durability in the outside environment, and then efficient membrane fusion during entry into the target cell. It is therefore reasonable to speculate that the virus adopts a different set of physical properties at different stages of its life cycle.

In this study we analyze the mechanical properties of HIV particles using nanoindentation experiments conducted by an atomic force microscope (AFM). The AFM has been successfully used to measure the mechanical properties of another retrovirus, Moloney murine leukemia virus (MLV) (12), as well as CAs of bacteriophage (13), cowpea chlorotic mottle virus (14), and minute virus (15). We show that the HIV maturation process is accompanied by a dramatic softening of the virion surface. This ''stiffness switch'' is an example of a complex macromolecular assembly drastically altering its mechanical properties by spontaneous internal

Submitted July 23, 2006, and accepted for publication November 21, 2006.

Address reprint requests to Itay Rousso, Dept. of Structural Biology, Weizmann Institute of Science, Rehovot 76100, Israel. Tel.: 972-8-9343479; Fax: 972-8-9344136; E-mail: itay.rousso@weizmann.ac.il; or Michael S. Kay, Dept. of Biochemistry, University of Utah School of Medicine, 15 N. Medical Drive East Rm. 4100, Salt Lake City, UT 84112-5650. Tel.: 801-585-5021; Fax: 801-581-7959; E-mail: kay@biochem.utah.edu.

0006-3495/07/03/1777/07 $2.00

doi: 10.1529/biophysj.106.093914

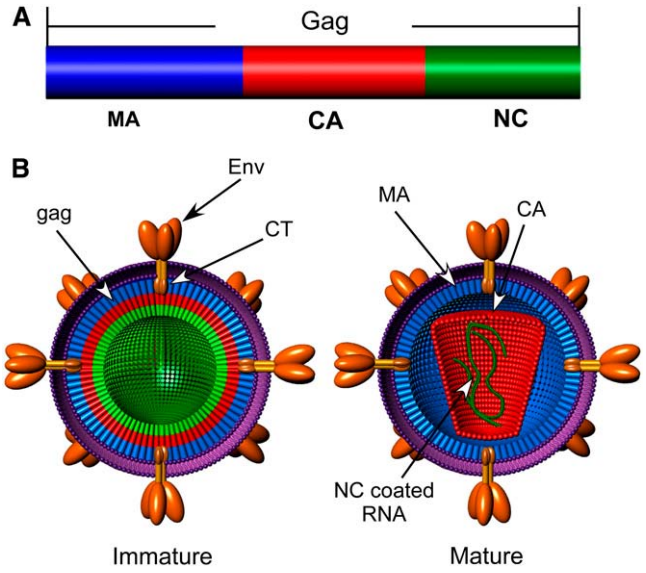

FIGURE 1 (*A*) Schematic representation of HIV Gag protein domains. MA (*blue*); CA (*red*); NC (*green*). For simplicity, other Gag domains, such as p2 and p6, that are not structural proteins are not shown. (*B*) Schematic models for HIV mature and immature states. In the immature form, a thick protein shell (~25 nm) composed of Gag is observed beneath the membrane. Viral maturation is induced by the proteolytic processing of Gag into three major structural domains: MA, CA, and NC. The mature HIV particle has a thin protein shell (~5 nm) and conical core. Maturation has no effect on the virus dimensions; both mature and immature particles have a diameter of ~100 nm. Env trimers are shown on the surface of the virion and do not undergo proteolytic processing during maturation. The Env ectodomain is in brown, and the transmembrane and CT domains are in tan.

rearrangement. Recently, HIV maturation was shown to affect the ability of virus particles to enter target cells (16,17) using a fluorescence-based assay (18). The entry activity of immature particles is almost 10-fold lower than that of mature particles. Truncation of the viral envelope protein (Env) CT domain restores the entry ability of immature virus particles (16,17). Strikingly, here we show that viral entry activity correlates with its mechanical changes, providing the first evidence, to our knowledge, of a link between mechanical and biological properties of a virus. These results show that HIV regulates its mechanical properties at different stages of its life cycle (i.e., stiff during viral budding versus soft during entry), and this regulation may be important for efficient infectivity.

MATERIALS AND METHODS

Virus preparation

Pseudovirion particles used in this study were produced by cotransfection of 293T cells with an ΔEnv HIV-1 genome containing an inactivating integrase mutant (DHIV3-GFP-D116G (19), provided by V. Planelles) and an Env expression vector (pEBB-HXB2 (20), provided by B. Chen). Immature particles were produced by cloning Gag with all PR sites deleted (pNL-MA/p6 (17), provided by C. Aiken) into the ΔEnv, Int^- HIV-1 genome. ΔCT HXB2 Env (Δ147 (6)) was provided by E. Hunter and cloned into pEBB-HXB2. Virus particles were collected and purified by centrifugation through a sucrose cushion (20% sucrose in TNE buffer: 0.1 M NaCl, 1 mM EDTA, 10 mM Tris, pH 7.6) at 20,000 × *g* for 90 min at 4°C. Virus pellets were then resuspended in TNE buffer. During all measurements, virus particles were kept in a physiological buffer (TNE). Purified viruses were attached to microscope glass slides that were pretreated with hexamethyldisilazane (HMDS) vapors. Western blots were developed using sheep polyclonal anti-gp120 (contributed by M. Phelan, National Institutes of Health AIDS Research and Reference Reagent Program) and rabbit polyclonal anti-CA (provided by W. Sundquist). Blots were quantified using Li-Cor's Odyssey instrument (Lincoln, NE).

Sample preparation for AFM imaging and force measurements

Microscope glass slides were cleaned by boiling in HCl solution, dried, and then incubated overnight in HMDS vapors to enable virus particles attachment (13). Before depositions, purified virus solutions were filtered through a 0.45-μm filter. A 10-μl droplet of virus supernatant was then deposited onto a glass slide and left to absorb to the substrate for 15 min. The glass surface was then rinsed with TNE buffer to remove unbound material. All measurements were carried out under TNE buffer.

Virus entry assays

HIV entry assays were performed essentially as described (17). Briefly, HIV particles were incubated with HOS-CD4-CXCR4 cells (provided by Benjamin Chen) for 2 h at 37°C. After removing unbound virus, entry events were detected using CCF2-AM dye (Invitrogen, Carlsbad, CA) as described in the manufacturer's instructions. Fluorescence was detected using a PolarStar Optima (BMG LABTECH, Offenburg, Germany) plate reader.

AFM imaging and indentation experiments

All AFM experiments were carried out using a Bioscope with a Nanoscope IV controller (Veeco, Santa Barbara, CA) equipped with a dimension XY closed loop scanner mounted on an inverted optical microscope (Axiovert 200M, Carl Zeiss AG, Jena, Germany). Images of virus particles were acquired in AFM tapping mode in a fluid environment and rendered using the WSxM software (Nanotec Electronica, Madrid, Spain, http://www.nanotec.es/progcorn.htm). Pyramidal silicon nitride probes (with a measured averaged stiffness of 0.22 N/m (DNP, Veeco) or 1.55 N/m (NSC36, Micromasch, Tallin, Astonia) were used, their spring constants being determined experimentally by measuring the thermal fluctuations of the cantilevers (21). Both probe types have a nominal tip radius of 20 nm. To measure the mechanical properties of an individual virus, an indentation experiment was performed with the microscope operated in the force-distance (FD) mode. Before beginning an indentation experiment, the probe was positioned at the center of the virus surface, and the AFM operation was switched from tapping to contact mode by reducing the driving amplitude to 0 mV. For each virus measurement, ~100 FD curves were performed at a scan rate of 0.5 Hz.

Data analysis for calculating the virus point stiffness

To obtain the measured point stiffness of a virus particle from a set of roughly 100 successive FD curves, each curve was shifted, first along the *z* axis to set the tip-sample contact point to a distance of zero, and then along the *y* axis to set the deflection in the noncontact region to zero. We further analyzed each experiment by plotting the individual measured point stiffness as a histogram and as a function of the measurement count (see Fig. 3 *B*). Virus measured stiffness (k_{meas}) was derived mathematically from the slope

of the FD curve. A linear function was fitted to the upper 75% of the FD curve (see Fig. 3 *A*). Virus particles whose point stiffness values decreased consistently during experimentation were discarded, since they underwent irreversible deformation, probably due to fatigue or even breakage. Next, a maximal deflection threshold value was set. Curves failing to reach this value were discarded, and the remaining aligned curves were averaged. The averaged FD curves were then converted from deflection units (V) to loading force (N) by multiplying by the deflection sensitivity (in nm/V, derived from a FD curve performed on mica) and the spring constant (N/m) of the cantilever. Virus measured stiffness (k_{meas}, in N/m) was derived mathematically from the slope of the averaged FD curve as described above. The stiffness of the virus (k_{virus}) was computed according to Hooke's law on the assumption that our experimental system can be modeled as two springs (the virus and the cantilever) arranged in series:

$$k_{virus} = \frac{k_{can} \times k_{meas}}{k_{can} - k_{meas}}.$$

Data analysis was carried out using MATLAB software (The MathWorks, Natick, MA). To calculate the Young's modulus from the measured virus stiffness, we utilized the finite element method as previously described (12).

RESULTS AND DISCUSSION

Native virus particles were imaged in a physiological buffer with the AFM operating in tapping mode to minimize possible damage. Under these imaging conditions, virus particles maintained their native dimensions, as determined by their cross sectional profiles. In addition, all of the virus particle types used in this study were found to have similar size (Fig. 2). We analyzed the point stiffness of viral particles by measuring FD curves, as shown in Fig. 3 *A*, for a mature HIV particle (FD curves for immature HIV particles are available online as Supplementary Material). As seen in Fig. 3 *A*, even at the maximal loading force, indentation depths are well below 10% of the sample thickness—the indentation limit determined by Bueckle's law (22), above which the rigid supporting substrate begins to contribute to the measured stiffness. Low penetration depths are essential for minimizing damage to the virus during the experiment and also ensure that the CA core (in the mature state) will not contribute significantly to the measured stiffness. The measured stiffness values derived from ~100 FD curves are plotted as a histogram to which a Gaussian curve is fitted (Fig. 3 *B*). During each experiment, the measured stiffness values derived from the individual FD curves were found to distribute normally around a mean without systematic deviation upon repeated measurements (Fig. 3 *B*, *inset*), which suggests that the virus did not undergo irreversible deformation during measurement.

The point stiffness measured for mature HIV particles is 0.22 ± 0.01 N/m ($n = 37$) (Fig. 4). Strikingly, immature particles are more than 14-fold stiffer, with a point stiffness of 3.15 ± 0.09 N/m ($n = 26$). To test if Env, the other major structural protein of HIV, might be contributing to the large difference in stiffness between the mature and immature virions, we measured HIV particles lacking Env (ΔEnv). The

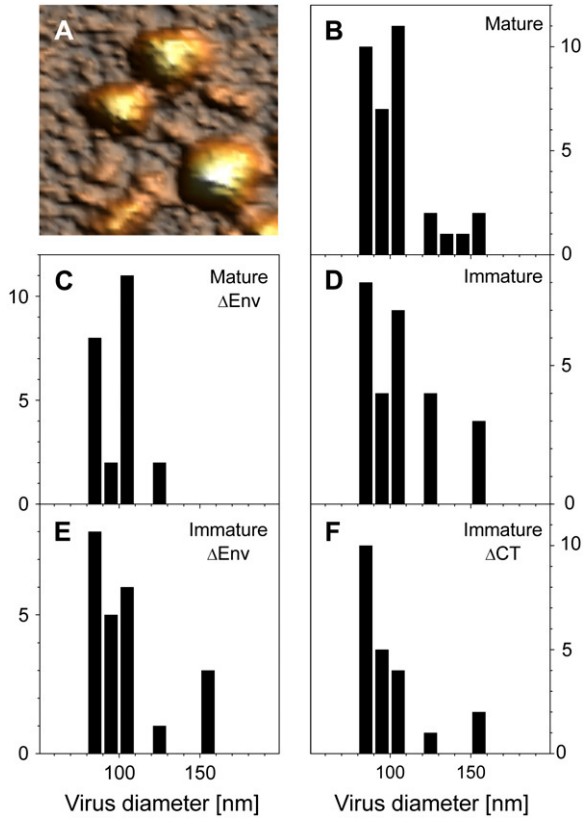

FIGURE 2 HIV particle shape and dimensions. (*A*) An AFM topographic image, acquired in tapping mode, of mature HIV virus in TNE buffer (scan area 3 × 3 μm, 170 × 170 pixels). Height distributions of mature virus particles (*B*), mature lacking Env particles (*C*), immature virus (*D*), immature lacking Env particles (*E*), and immature particles lacking the CT domain (*F*). The corresponding averaged heights in nanometers are 98 (SD = 12, $n = 23$), 94 (SD = 22, $n = 26$), 101 (SD = 23, $n = 23$), 98 (SD = 21, $n = 22$). Virus size was determined by height rather than width, because the width of the virus is larger and less accurate due to convolution between the AFM tip and the virus.

presence of Env in mature HIV particles has little effect on stiffness (ΔEnv is 0.21 ± 0.01 N/m ($n = 24$) vs. 0.22 N/m with Env). In contrast, ΔEnv immature particles have a dramatically decreased stiffness (0.52 ± 0.02 N/m ($n = 23$)) compared to immature particles with Env (3.15 N/m) (Fig. 4). These ΔEnv immature particles are still more than twice as stiff as mature particles (with or without Env) but are more than sixfold softer than Env-containing immature viruses. Previous cryo-EM studies of HIV particles show that the protein shell of the immature form is nearly five times thicker than the mature form, and this thickness is not affected by the presence of Env (23). Based on EM analysis as well as our previous MLV study (12), we expected that a virus with a thicker protein shell will be stiffer than one with a thinner shell. Our current results indicate that, in fact, the impact of the protein shell thickness (mature ΔEnv versus immature ΔEnv) is much smaller than of Env on virus stiffness (immature with versus without Env). Env likely does not have an appreciable impact on mature virus stiffness since

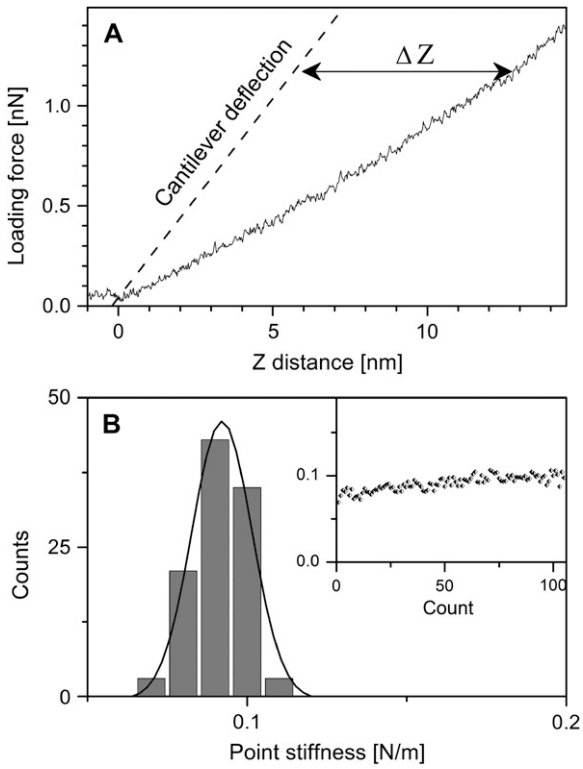

FIGURE 3 Measuring the point stiffness of the virus by indentation type experiments. (*A*) Typical force distance curve for a mature virus attached to HMDS-pretreated glass slide (*solid line*) and the deflection of the cantilever (*dotted black line*). Curves were shifted along the *z* axis to set the tip-sample contact point (Z_0) to a distance of zero. For each experiment, ~100 curves were acquired. The virus indentation depth is defined as the difference between the *z* position of the virus and cantilever deflection at a given loading force (labeled as ΔZ). (*B*) A histogram, over which a normal distribution curve is fitted, of the individual measured point stiffness values derived from the consecutive force distance curves. The inset shows the individual measured point stiffness values obtained for a virus during a single measurement against the experiment number (count). These plots, together with the observed distribution of the individual measured spring constants, demonstrate that the virus did not undergo significant irreversible deformation during the indentation measurements.

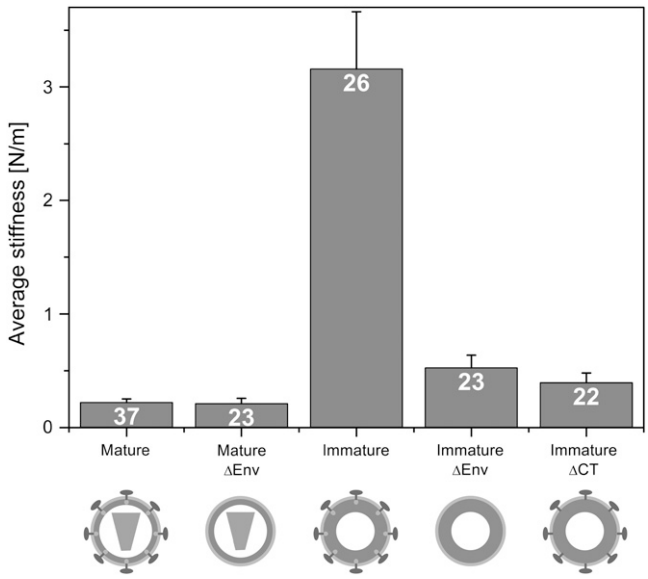

FIGURE 4 Averaged point stiffness of HIV virus. Each value was calculated from the average of ~100 FD curves obtained from individual virus particles. The bars represent the standard error of the mean, and the number of virions analyzed is indicated by the number shown within each column. The distribution of the measured point stiffness values as well as the stiffness as a function of the virus particles' diameter are available online as Supplementary Material.

the Gag-Env interaction is broken during maturation by the proteolytic processing of Gag.

To determine if the HIV CT domain mediates the stiffening of immature virions, we measured the stiffness of immature particles with Env lacking the CT domain (ΔCT). ΔCT virions incorporate a normal amount of Env because of high surface expression (caused by the loss of an endocytosis signal in the CT domain (24–26)). As seen in Fig. 4, the point stiffness of immature ΔCT HIV particles is 0.39 ± 0.01 N/m ($n = 22$), similar to the ΔEnv immature particles (0.52 N/m). Thus, the CT domain appears to be the main contributor to the greatly increased rigidity of the immature state.

The Young's modulus is an inherent material property that in contrast to point stiffness does not depend on the geometry of the sample. Thus, it provides an insight into the average interactions between the building blocks of the virus supramolecular shell. To estimate the average Young's moduli (E) of virus particles from the measured virus stiffness, we described the mechanical behavior of the virus as a homogenous, linear elastic material. Within this framework we have modeled our indentation experiments by using a finite element method as previously described by Kol et al. (12). All virus particle types were modeled as hollow spheres with an outer radius of 50 nm and inner radius of 45 and 25 nm for the mature and immature states, respectively. Virus dimensions were adopted from an HIV electron cryomicroscopy study (23). The calculated Young's modulus values are listed in Table 1.

Finite element simulation (FES) provides further support for the role of Env CT in stabilizing the immature virus protein shell as indicated by the ~8-fold increase in the average Young's modulus when the CT domain is present (115 vs. 930 MPa).

The number of Env trimers (and therefore, Env CT domains) on the surface of an HIV particle is currently controversial but is thought to be low (7–72 trimers, (27–32)). The dramatic effect these relatively small numbers of Env trimers exert on the global stiffness of an ~100 nm viral particle is remarkable. To exclude the possibility that this large and unexpected Env effect is due to overincorporation of Env, we confirmed by Western blot analysis that the level of Env incorporation into the pseudotyped virions used in this study is similar or less than that of authentic virions (with Env contained in the viral genome, data not shown).

TABLE 1 The mechanical properties of HIV particles

State	R_{ext} [nm]	Wall thickness [nm]	K [N/m]	Estimated E [MPa]
Mature	50	5	0.22	440
Immature	50	25	3.16	930
Immature ΔCT	50	25	0.39	115

We have recently reported the effect of maturation on the mechanical properties of another retrovirus, MLV (12). Comparison between the properties of the two retroviruses provides two main observations: 1), The Young's modulus of mature HIV particles (440 MPa) is more than twofold lower than mature MLV (1.03 GPa) (12). This result suggests that the protein-protein interactions in the MLV mature shell are stronger that those in the HIV mature shell. 2), In sharp contrast to the dramatic stiffness switch observed here with HIV, MLV particles undergo a much more subtle (~2-fold) decrease in stiffness during maturation. The mature state of HIV and MLV virions have a very similar stiffness, whereas immature HIV is ~5-fold stiffer than immature MLV. Additionally, in our previous MLV mechanical analysis (12), we find that the Young's modulus of the mature state is ~4-fold higher than the immature state. Here we find that the Young's modulus of the HIV mature state is more than twofold lower than the immature state. Interestingly, the changes in MLV stiffness and Young's modulus with maturation are quite similar to those we observe between HIV mature and ΔCT immature virions. The difference in stiffness between the HIV and MLV immature forms can be explained by the fact that MLV is not a lentivirus and thus does not possess a long CT domain. Alternatively, the difference may be rationalized by the presence of a poorly ordered layer in the MLV immature shell, the pp12 domain (33), localized between the MA and CA domains, which is likely to destabilize the shell of the MLV immature state. Such a poorly ordered domain is not present in HIV Gag.

The dramatic effect of Env on the virus stiffness may be explained by the following two possibilities: a), Interactions between Env (via CT) and Gag (via MA) at positions on the virus protein shell propagate throughout the Gag layer to stabilize the entire shell; and alternatively b), the assembly of Gag proteins during viral formation may depend on Env CT. In the absence of Env CT, Gag proteins may self-assemble into a different structural arrangement that is less stable than the organization of Gag formed when Env CT is present, which is manifested as decreased stiffness.

To correlate virus mechanical properties and biological activity, we measured the entry activity of virus particles used in this work using a fluorescence-based assay (18). In agreement with previously reported results (17,34), we find that immature virus particles enter target cells very inefficiently, but truncation of the Env CT domain rescues their entry ability (Fig. 5). These results correlate well with the stiffness of the virus shell. Soft mature virus particles can enter cells efficiently, whereas the stiffer immature form cannot. Removal of the Env CT domain in the immature virus dramatically softens the virus shell and restores the entry activity of these particles.

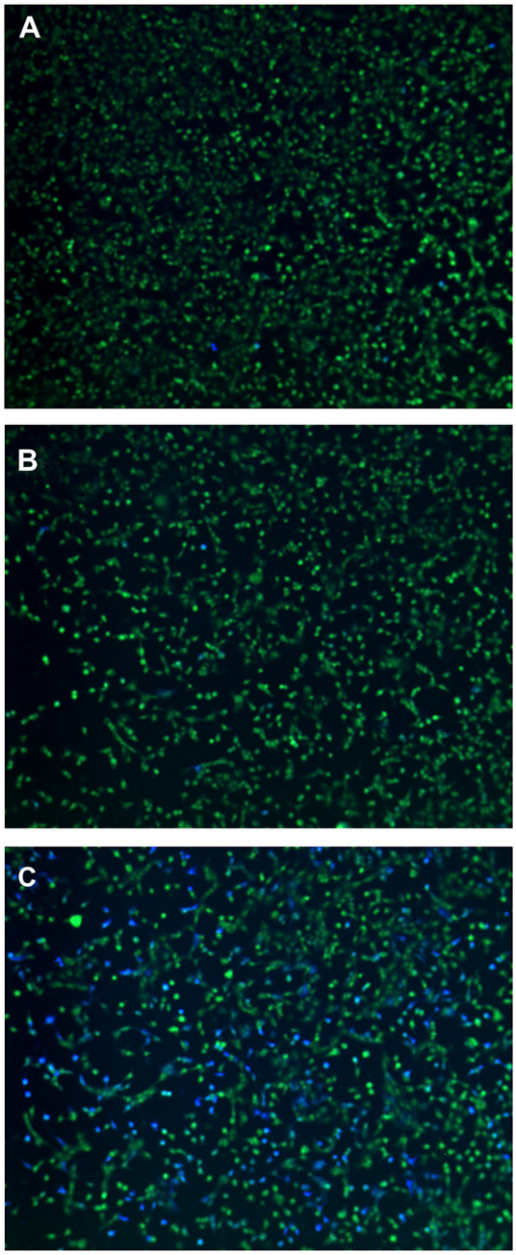

FIGURE 5 Viral reporter particle entry assay. Viruses are packaged with a Vpr-β-lactamase fusion protein. HOS-CD4-CXCR4 cells are loaded with GeneBlazer dye (Invitrogen), which is cleaved by β-lactamase upon viral entry (causing a green to blue shift in fluorescence). Blue cells indicate entry events. Shown are fluorescence micrographs of (*A*) uninfected cell control, (*B*) immature virions with wild-type Env, and (*C*) immature virions with ΔCT Env. The results are representative of at least two independent experiments.

These results show that the very high stiffness of immature HIV particles depends on the presence of the Env CT domain, whereas the thickness of the protein shell plays a

much smaller role. Intriguingly, we find a strong correlation between virus stiffness and its ability to enter target cells. Recently, we provided evidence that mature MLV virus particles have an elastic and brittle shell and postulated that this shell undergoes deformation during fusion (12). Based on our results, we speculate that immature virions cannot enter cells efficiently because their shell is too stiff to easily undergo deformation. The entry ability of virus particles will likely also depend on additional factors, such as changes in the conformation of Env related to its CT domain (''inside-out'' signaling (16,17)) and the lateral diffusion of Env trimers in the membrane.

In summary, our discovery of an Env-mediated stiffness switch that correlates with viral entry activity provides, to our knowledge, the first evidence for a possible role of virus mechanical properties in the infection process. This work establishes the groundwork for future mechanistic studies on virus self-assembly and, more generally, how biological systems regulate their mechanical properties, as well as how this regulation can be employed to control biological function.

SUPPLEMENTARY MATERIAL

An online supplement to this article can be found by visiting BJ Online at http://www.biophysj.org.

I.R. is the incumbent of the Robert Edwards and Roselyn Rich Manson Career Development Chair. We thank C. Aiken, D. Eckert, C. Hill, W. Sundquist, and S. Weiner for discussions and critical review of the manuscript.

This work was supported in part by the Jean-Jacques Brunschwig Fund for the Molecular Genetics of Cancer (I.R.), the Kimmelman Center for Macromolecular Assemblies (I.R.), and the National Institutes of Health (M.K.).

REFERENCES

1. Wills, J. W., and R. C. Craven. 1991. Form, function, and use of retroviral Gag proteins. *AIDS*. 5:639–654.
2. Berger, E. A., P. M. Murphy, and J. M. Farber. 1999. Chemokine receptors as HIV-1 coreceptors: roles in viral entry, tropism, and disease. *Annu. Rev. Immunol.* 17:657–700.
3. Chan, D. C., and P. S. Kim. 1998. HIV entry and its inhibition. *Cell.* 93:681–684.
4. Freed, E. O., and M. A. Martin. 1995. Virion incorporation of envelope glycoproteins with long but not short cytoplasmic tails is blocked by specific, single amino acid substitutions in the human immunodeficiency virus type 1 matrix. *J. Virol.* 69:1984–1989.
5. Moore, J. P., and J. Binley. 1998. HIV. Envelope's letters boxed into shape. *Nature.* 393:630–631.
6. Dubay, J. W., S. J. Roberts, B. H. Hahn, and E. Hunter. 1992. Truncation of the human immunodeficiency virus type 1 transmembrane glycoprotein cytoplasmic domain blocks virus infectivity. *J. Virol.* 66:6616–6625.
7. Freed, E. O., and M. A. Martin. 1995. The role of human immunodeficiency virus type 1 envelope glycoproteins in virus infection. *J. Biol. Chem.* 270:23883–23886.
8. Freed, E. O., and M. A. Martin. 1996. Domains of the human immunodeficiency virus type 1 matrix and gp41 cytoplasmic tail required for envelope incorporation into virions. *J. Virol.* 70:341–351.
9. Spies, C. P., G. D. Ritter Jr., M. J. Mulligan, and R. W. Compans. 1994. Truncation of the cytoplasmic domain of the simian immunodeficiency virus envelope glycoprotein alters the conformation of the external domain. *J. Virol.* 68:585–591.
10. Swanstrom, R., and J. W. Wills. 1997. Synthesis, assembly, and processing of viral proteins. *In* Retroviruses. J. M. Coffin, S. H. Hughes, and H. E. Varmus, editors. Cold Spring Harbor Laboratory Press, Plainview, NY. 263–334.
11. Coffin, J. M., S. H. Hughes, and H. E. Varmus, editors. 1997. Retroviruses. Cold Spring Harbor Laboratory Press, Plainview, NY.
12. Kol, N., M. Gladnikoff, D. Barlam, R. Z. Shneck, A. Rein, and I. Rousso. 2006. Mechanical properties of murine leukemia virus particles. Effect of maturation. *Biophys. J.* 91:767–774.
13. Ivanovska, I. L., P. J. de Pablo, B. Ibarra, G. Sgalari, F. C. MacKintosh, J. L. Carrascosa, C. F. Schmidt, and G. J. Wuite. 2004. Bacteriophage capsids: tough nanoshells with complex elastic properties. *Proc. Natl. Acad. Sci. USA.* 101:7600–7605.
14. Michel, J. P., I. L. Ivanovska, M. M. Gibbons, W. S. Klug, C. M. Knobler, G. J. Wuite, and C. F. Schmidt. 2006. Nanoindentation studies of full and empty viral capsids and the effects of capsid protein mutations on elasticity and strength. *Proc. Natl. Acad. Sci. USA.* 103:6184–6189.
15. Carrasco, C., A. Carreira, I. A. Schaap, P. A. Serena, J. Gomez-Herrero, M. G. Mateu, and P. J. de Pablo. 2006. DNA-mediated anisotropic mechanical reinforcement of a virus. *Proc. Natl. Acad. Sci. USA.* 103:13706–13711.
16. Murakami, T., S. Ablan, E. O. Freed, and Y. Tanaka. 2004. Regulation of human immunodeficiency virus type 1 Env-mediated membrane fusion by viral protease activity. *J. Virol.* 78:1026–1031.
17. Wyma, D. J., J. Jiang, J. Shi, J. Zhou, J. E. Lineberger, M. D. Miller, and C. Aiken. 2004. Coupling of human immunodeficiency virus type 1 fusion to virion maturation: a novel role of the gp41 cytoplasmic tail. *J. Virol.* 78:3429–3435.
18. Cavrois, M., C. De Noronha, and W. C. Greene. 2002. A sensitive and specific enzyme-based assay detecting HIV-1 virion fusion in primary T lymphocytes. *Nat. Biotechnol.* 20:1151–1154.
19. Dehart, J. L., J. L. Andersen, E. S. Zimmerman, O. Ardon, D. S. An, J. Blackett, B. Kim, and V. Planelles. 2005. The ataxia telangiectasia-mutated and Rad3-related protein is dispensable for retroviral integration. *J. Virol.* 79:1389–1396.
20. Chen, B. K., K. Saksela, R. Andino, and D. Baltimore. 1994. Distinct modes of human immunodeficiency virus type 1 proviral latency revealed by superinfection of nonproductively infected cell lines with recombinant luciferase-encoding viruses. *J. Virol.* 68:654–660.
21. Hutter, J. L., and J. Bechhoefer. 1993. Calibration of atomic-force microscope tips. *Rev. Sci. Instrum.* 64:1868–1873.
22. Bueckle, H. 1973. Use of hardness to determine other material properties. *In* The Science of Hardness Testing and Its Research Applications. J. W. Westbrook and H. Conrad, editors. American Society for Metals, Materials Park, OH.
23. Wilk, T., I. Gross, B. E. Gowen, T. Rutten, F. de Haas, R. Welker, H. G. Krausslich, P. Boulanger, and S. D. Fuller. 2001. Organization of immature human immunodeficiency virus type 1. *J. Virol.* 75:759–771.
24. Berlioz-Torrent, C., B. L. Shacklett, L. Erdtmann, L. Delamarre, I. Bouchaert, P. Sonigo, M. C. Dokhelar, and R. Benarous. 1999. Interactions of the cytoplasmic domains of human and simian retroviral transmembrane proteins with components of the clathrin adaptor complexes modulate intracellular and cell surface expression of envelope glycoproteins. *J. Virol.* 73:1350–1361.
25. Boge, M., S. Wyss, J. S. Bonifacino, and M. Thali. 1998. A membrane-proximal tyrosine-based signal mediates internalization of the HIV-1 envelope glycoprotein via interaction with the AP-2 clathrin adaptor. *J. Biol. Chem.* 273:15773–15778.
26. Rowell, J. F., P. E. Stanhope, and R. F. Siliciano. 1995. Endocytosis of endogenously synthesized HIV-1 envelope protein. Mechanism and role in processing for association with class II MHC. *J. Immunol.* 155:473–488.

27. Chertova, E., J. W. Bess Jr., B. J. Crise, I. R. Sowder, T. M. Schaden, J. M. Hilburn, J. A. Hoxie, R. E. Benveniste, J. D. Lifson, L. E. Henderson, and L. O. Arthur. 2002. Envelope glycoprotein incorporation, not shedding of surface envelope glycoprotein (gp120/SU), is the primary determinant of SU content of purified human immunodeficiency virus type 1 and simian immunodeficiency virus. *J. Virol.* 76: 5315–5325.

28. Gelderblom, H. R. 1991. Assembly and morphology of HIV: potential effect of structure on viral function. *AIDS.* 5:617–637.

29. Hockley, D. J., R. D. Wood, J. P. Jacobs, and A. J. Garrett. 1988. Electron microscopy of human immunodeficiency virus. *J. Gen. Virol.* 69:2455–2469.

30. Ozel, M., G. Pauli, and H. R. Gelderblom. 1988. The organization of the envelope projections on the surface of HIV. *Arch. Virol.* 100: 255–266.

31. Zhu, P., E. Chertova, J. Bess Jr., J. D. Lifson, L. O. Arthur, J. Liu, K. A. Taylor, and K. H. Roux. 2003. Electron tomography analysis of envelope glycoprotein trimers on HIV and simian immunodeficiency virus virions. *Proc. Natl. Acad. Sci. USA.* 100:15812–15817.

32. Zhu, P., J. Liu, J. Bess Jr., E. Chertova, J. D. Lifson, H. Grise, G. A. Ofek, K. A. Taylor, and K. H. Roux. 2006. Distribution and three-dimensional structure of AIDS virus envelope spikes. *Nature.* 441: 847–852.

33. Yeager, M., E. M. Wilson-Kubalek, S. G. Weiner, P. O. Brown, and A. Rein. 1998. Supramolecular organization of immature and mature murine leukemia virus revealed by electron cryo-microscopy: implications for retroviral assembly mechanisms. *Proc. Natl. Acad. Sci. USA.* 95:7299–7304.

34. Jiang, J., and C. Aiken. 2006. Maturation of the viral core enhances the fusion of HIV-1 particles with primary human T cells and monocyte-derived macrophages. *Virology.* 346:460–468.